

Magnetoconductance fluctuations in mesoscopic spin glasses

Marek Cieplak

Institute of Physics, Polish Academy of Sciences, PL 02-668 Warsaw, Poland

B. R. Bulka

Institute of Molecular Physics, Polish Academy of Sciences, PL 60-179 Poznan, Poland

T. Dietl

Institute of Physics, Polish Academy of Sciences, PL 02-668 Warsaw, Poland

(Received 14 June 1994)

Results of numerical studies of conductance of a two-dimensional tight-binding system with random potentials and coupled to a three-dimensional Ising spin glass are presented. The dynamics of the systems are determined by the Monte Carlo process of the Ising spins. The paper is focused on the effects of the magnetic field which couples to the lattice spins and changes their configuration. The conductance noise in the presence of the field is given by a power law, like in the absence of the field. The magnetoconductance fluctuations, obtained from studying time-averaged trains of conductance for a given field, increase in amplitude on lowering temperature. This is unlike what happens with the thermal noise and with what happens with magnetoconductance fluctuations in spin ferromagnets. The dependence of conductance on the magnetic field depends on the size of the field increments and on the starting spin configuration. It depends also, to a lesser degree, on the time interval used in averaging. The field-cycling magnetoconductance curves are not reproducible. Experimental results, on the other hand, are, to a large extent, reproducible. Possible reasons for this discrepancy are discussed.

I. INTRODUCTION

Manifestations of quantum interference effects in mesoscopic electronic systems can be used to study structures and processes in solids at the microscopic level.^{1,2} One natural possibility is to probe spin dynamics, as suggested by Altshuler and Spivak.³ It is especially interesting to try this approach in the case of spin glasses. Feng *et al.*⁴ have proposed that the chaotic nature of spin reorganizations on varying temperature T , would result in measurable changes of conductance noise. Experimental studies of such noise⁵ have not yet come up with an evidence for the changes, possibly due to nonlinearity of the strong current conditions required to measure the noise. Neither the numerical simulations⁶ gave any indication of a promise to measure chaos this way, possibly due to too small system sizes available to numerical studies. Nevertheless all these studies are merely first steps toward interpreting experimental information being gathered on mesoscopic systems with spins.

This paper is meant to be a sequel to our former theoretical studies⁶ of the conductance noise and is now focused on magnetoconductance and irreversibilities related to the effect of magnetic field on the lattice spins. Measuring magnetoconductance appears easier than determining noise and there are several groups which work on this.⁷⁻¹¹ Most of the experimental studies refer to systems in which both the lattice spins and the conduction electrons are located in three-dimensional (3D) space. However, the dilute semiconducting systems studied in Poland^{8,12,13} are likely to be easier for a theorist: the conduction process there takes place within a 200-Å-

wide layer adjacent to a grain boundary and is thus essentially of a 2D nature whereas the lattice spins form a 3D system. This mixed-dimensionality electron-spin system is our object of studies here and the details of the model are presented in Sec. II. The model consists basically of a 3D spin glass made of Ising spins a layer of which is coupled to a 2D tight-binding electron with spin, moving in a random potential.

It should be noted that experiments are usually performed in a four-probe geometry, such as analyzed theoretically by Hershfield.¹⁴ Our simulations, however, use a two-probe arrangement: there are two perfect leads attached to a random segment. This is done for two reasons. First, our calculation of conductance is based on iterations of Green functions which is numerically exact but restricted to small system sizes: carving out space for two more leads, in the simulated systems, is difficult. Second, one should attempt to understand the simplest geometry first.

When it comes to studying effects of the magnetic field B , a theoretical analysis allows one to split the coupling of the field to the system into three mechanisms: alignment of the lattice spins (lattice Zeeman effect), alignment of the electronic spins (electronic Zeeman), and modification of phases of the electronic wave functions (orbital effects). As recently shown by de Vegvar and Fulton,¹⁵ it is possible to separate the spin and orbital effects experimentally. In this paper, we focus on the lattice Zeeman coupling. In particular, we examine how field-induced changes in the spin configurations affect the conductance.

Presentation of our results starts in Sec. III where we

study in what ways the conductance noise is affected by the presence of a magnetic field and we advance interpretation of the noise in terms of spin flips. In Sec. IV we discuss issues related to defining magnetoconductance. The lattice spin subsystem undergoes the Monte Carlo dynamics which produce effective time-dependent tight-binding potentials. In order to define conductance for a given B one has to time average over the instantaneous values. The resulting conductance depends on the coarse-graining time interval, i.e., on the measuring apparatus. Our studies indicate, at least for short time scales, that this dependence is weak. The dependencies on the value of B , on the way B is incremented, and finally on the initial spin configurations are much stronger.

In Sec. V, we study the T dependence of the rms fluctuations as a function of B and contrast it to that predicted for ferromagnets and to the behavior of the rms fluctuations generated as a function of time. The predicted increase in the amplitude of magnetoconductance fluctuations on cooling of spin glasses appears to agree qualitatively with the findings of de Vegvar *et al.*^{7,15} (who plot a linear combination of four-probe resistivities obtained for fields B and $-B$). In Sec. VI, we demonstrate that field cycling is irreversible: the field-up magnetoconductance curve is uncorrelated with the field-down curve. Similarly, increasing and decreasing B away from some origin again produces uncorrelated curves. Experimentally, however, a good deal of reversibility is actually observed.^{7,8,11,12} We offer several possibilities to explain this.

II. DESCRIPTION OF THE SYSTEM

As in our previous paper,⁶ we define the system by the Hamiltonian

$$\mathcal{H} = H_s + H_{e-s} + H_e, \quad (1)$$

where H_e describes electrons hopping on a two-dimensional square lattice, H_s describes the three-dimensional spin-glass system, and H_{e-s} corresponds to the interaction between the two subsystems.

We take the lattice spins to occupy sites of the $L_s \times L_s \times L_s$ cubic lattice, with $L_s = 9$. A central plane in this lattice coincides with the plane on which the tight-binding system is defined but the spin lattice forms a superlattice on the lattice of the disordered potentials.

The spin Hamiltonian is given by

$$H_s = - \sum_{\langle i,j \rangle} J_{ij} S_i S_j + g_s \mu_B B \sum_i S_i, \quad (2)$$

where S_i are Ising spins which take values ± 1 and J_{ij} is a random number distributed with the Gaussian probability with 0 mean and dispersion equal to J_0 . The spin-glass freezing temperature of this system is known to be close to J_0/k_B .^{16,17} In the Zeeman term, g_s is the lattice spin g factor. We introduce the shorthand notation

$$H = g_s \mu_B B / J_0 \quad (3)$$

to measure the lattice spin Zeeman energy in terms of the characteristic exchange energy. In practice, we shall

vary H between -1 and $+1$.

The effect of the magnetic field on the electrons is neglected and thus the electron Hamiltonian H_e can be expressed as

$$H_e = \sum_{l,a} \Psi_l^\dagger U(l,a) \Psi_{l+a} + \sum_l \Psi_l^\dagger V(l) \Psi_l, \quad (4)$$

where

$$\begin{aligned} \Psi_l^\dagger &= (c_{l+}^\dagger, c_{l-}^\dagger), \\ \Psi_l &= \begin{pmatrix} c_{l+} \\ c_{l-} \end{pmatrix} \end{aligned} \quad (5)$$

represent creation and annihilation operators for electrons at site l and spin states $+$ or $-$. The summation is over all sites of the square lattice.

The matrix U is given by

$$U(l,a) = \begin{pmatrix} u & 0 \\ 0 & u \end{pmatrix}, \quad (6)$$

where u is the hopping matrix element. The hopping is confined to the nearest-neighbor sites and vector $\mathbf{a} = (a_x, a_y)$ connects two such sites. For the square lattice $a_x, a_y = \pm 1$ in units of the lattice constant. The matrix V is defined by

$$V(l) = \begin{pmatrix} \epsilon(l) & 0 \\ 0 & \epsilon(l) \end{pmatrix}, \quad (7)$$

where $\epsilon(l)$ is the potential at site l .

We assume the following geometry for the electronic subsystem. Atomic sites lie on the square lattice. The central $L_x \times L_y$ section is disordered. In this section, potentials $\epsilon(l)$ are random. We chose them to be uniformly distributed between $-w/2$ and $w/2$, with $w = 2u$. Infinite perfect leads are attached in the x direction, to the left- and right-hand sides of the section. In the leads, $\epsilon(l) = 0$. Periodic boundary conditions are applied in the y direction. We typically study systems with $L_x = L_y = L = 20$. According to Stone,¹⁸ the universal conductance fluctuations actually show an L dependence which saturates for L close to and exceeding 20, hence the choice of our system size. The magnetic sites typically occupy only a fraction of the atomic sites and with $L_s = 9$ we have an arrangement in which every other site along each principal direction contains a lattice spin.

The coupling between the two subsystems is given by

$$H_{e-s} = -\frac{1}{2} J_{e-s} \sum_{\mathbf{m}} \Psi_{\mathbf{m}}^\dagger \boldsymbol{\sigma} \cdot \mathbf{S}_{\mathbf{m}} \Psi_{\mathbf{m}}, \quad (8)$$

where \mathbf{m} runs through those sites of the disordered segment which contain a lattice spin. We took $J_{e-s} = w/5$ so that the coupling acts as a small perturbation. $\boldsymbol{\sigma} = (\sigma^x, \sigma^y, \sigma^z)$ and σ^a are the Pauli matrices. In the present work we consider only Ising spins so only the σ^z term enters Eq. (7).

For a given configuration of the lattice spins the calculation of conductivity, σ , proceeds in exactly the same way as in Ref. 6 and it is based on the iterative evaluation of Green functions that enter the corresponding

Kubo formula.^{19–22} We focus on just one representative location of the Fermi energy: at $E=0$, which is close to a minimum in the σ vs E plot generated for a fixed spin configuration. Throughout the paper we consider only one sample, i.e., one particular choice of random potentials and of exchange couplings.

The time evolution of the system is determined by the Monte Carlo dynamics of the spin system. In each Monte Carlo step per spin, we pick $L_s \times L_s \times L_s$ sites, one at a time, and attempt to flip the spin there. This is governed by the Boltzmann factor corresponding to temperature T . The procedure probes short time scales since each Monte Carlo step corresponds, roughly, to 1 ps. In our simulations, we cool the system through the freezing temperature of $1 J_0/k_B$ by starting high up in the paramagnetic regime, at $T=3J_0/k_B$, and ending eventually at $0.4J_0/k_B$. At each T , the Monte Carlo process takes the system through 4500 steps per spin. The conductivity is being calculated for several selected temperatures. The first 2000 Monte Carlo steps are excluded from the calculations to improve thermal equilibration. After that the conductivities are determined at completion of each Monte Carlo step per spin. When studying the noise spectrum, we consider trains of 2^{12} conductivities. When studying the magnetoconductance, we cool the system at zero field and then increment the field in steps, allowing for a specified number of Monte Carlo steps for each field, as explained in Sec. IV.

III. CONDUCTANCE NOISE AND ITS RELATION TO SPIN EVENTS

We calculated the power spectra of the noise and averaged them over 20 realizations of 4096-long trains of data for the same sample, corresponding to different initial conditions. Figure 1 is for $T=0.8J_0/k_B$. The lighter symbols correspond to noise in the absence of the magnetic field, taken from Ref. 3, and the darker ones to

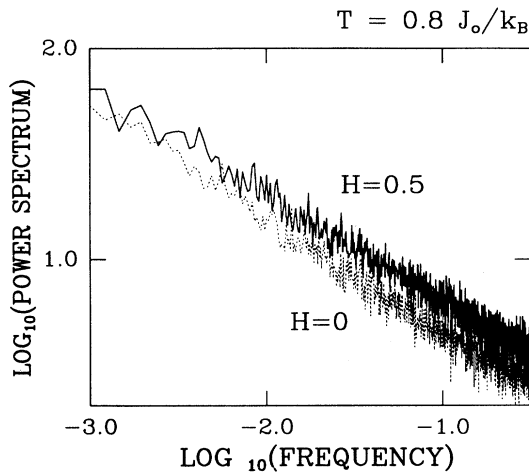


FIG. 1. Power spectrum on the log-log scale for $T=0.8J_0/k_B$. The lighter symbols are for $H=0$, and the darker ones for $H=0.5$, as indicated in the figure. This is a power-law noise, $f^{-\alpha}$, with $\alpha=0.5$.

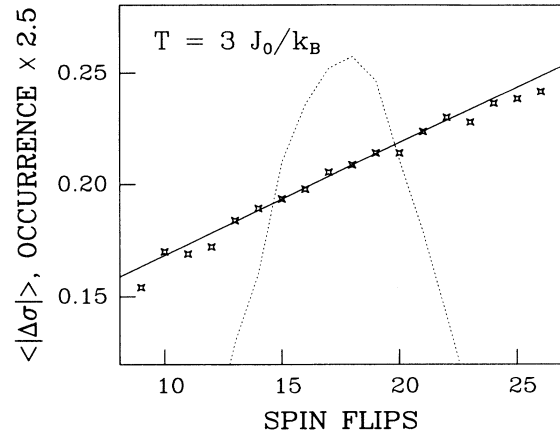


FIG. 2. The dotted line shows probability of a given the number of spin flips, N_f , that occurred in the central plane in a Monte Carlo step per spin at $T=3J_0/k_B$. $\langle N_f \rangle = 17.94$. The data points show average change in conductivity for a given N_f . The connecting solid line has a slope of 0.0047. Average N_f is linearly related to average $|\Delta\sigma|$.

noise generated when $H=0.5$. The field is applied only to the lattice spins here. In both cases we get a power-law noise with an exponent close to -0.5 . Clearly, the presence of H does not seem to change the nature of the noise. Only the noise amplitude is affected. Thus the microscopic processes with and without H (at the length scales studied) are essentially the same.

In our previous paper we have pointed out that jumps in conductivity are not uniquely correlated with the size of events in the spin system. Flipping many spins may result in a small change in conductivity and flipping few spins may have a major impact. Here, we want to point out, however, that a statistical correlation does exist: large spin events lead, on average, to larger changes in conductivity than small size spin events. This is shown in Fig. 2 where H was set equal to 0 for simplicity.

Note that the number of spin flips in the central plane varies from step to step. Its average grows with T roughly quadratically. The dotted line in Fig. 2 shows probability of having a given number of spins flipped at the largest T studied, i.e., at $3J_0/k_B$. The average size of the central plane events corresponds to flipping 17.94 spins at this T (the statistics are based on about 50 000 entries). The data points joined by the solid line show the average change in conductivity, $\langle |\Delta\sigma| \rangle$, for a given number of spin flips. These flips were generated during the runs and entries close to 17.94 have the largest statistical weight. Flips involving, say, 10 or 25 sites are in the tails of the probability distribution but even these data points agree with the linear law: $\langle |\Delta\sigma| \rangle \approx 0.0047N + \text{const.}$

IV. TIME-AVERAGING OF MAGNETOCONDUCTANCE

Any realistic measurement of conductance, σ , involves time coarse graining related to the resolution time scales of the apparatus. More importantly, a measurement of resistance corresponding to a single specific spin

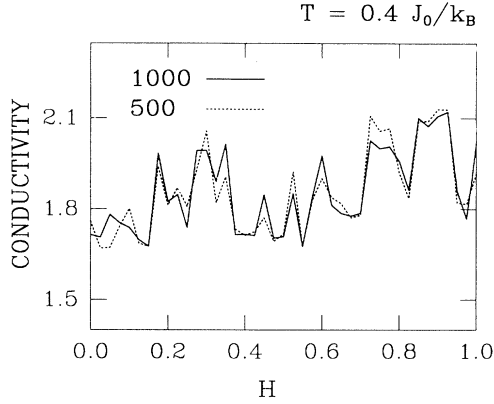


FIG. 3. Conductivity as a function of H for temperature $0.4J_0/k_B$. H is incremented in 40 steps. The conductance is averaged either over 1000 Monte Carlo steps per spin (solid line) or over 500 steps (dotted line).

configuration yields only a very weak imprint of temperature. Thus the instantaneous values of σ obtained for each Monte Carlo step per spin need to be averaged over a range of steps. We considered this range, Δt , to be equal to 500, 1000, and sometimes 2000 steps per spin.

Typical results are shown in Fig. 3. Here H is incremented in 40 stages from 0 to 1. We cool the system to $T=0.4J_0/k_B$ at $H=0$ and arrive at some “starting” spin configuration. We then put $H=0.025$, evolve the system for $(500+\Delta t)$ steps per spin, and then repeat the procedure with the next value of the field. The conductance is averaged over the last Δt steps in each stage. Figure 3 compares results obtained for $\Delta t=1000$ to those for $\Delta t=500$ to demonstrate existence of some sensitivity to the choice of Δt [going to $\Delta t=2000$ results in a still further modification of $\sigma(H)$]. This sensitivity, however, is minor compared to the other factors to be discussed

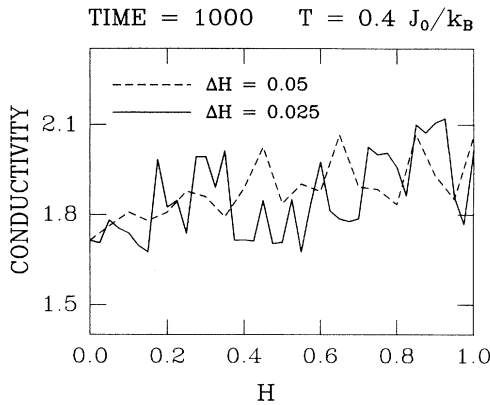


FIG. 4. Conductivity vs H for various way of incrementing H . The solid line is for a 40-step increase of H from 0 to 1. This is the solid line of Figs. 3 and 4. The dotted line is for a 20-step increase. Time 1000 at the left top of this and following figures indicates the value of Δt taken into the averaging process.

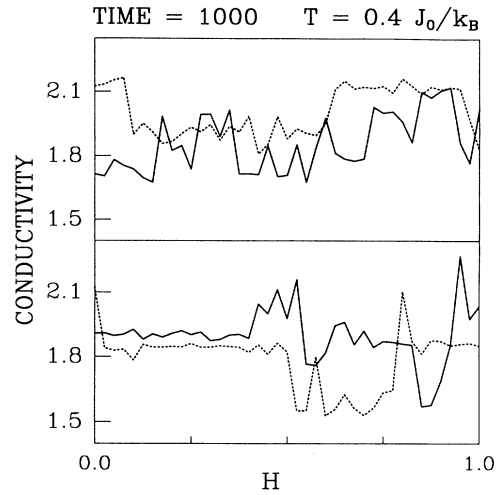


FIG. 5. Conductivity as a function of H for four different starting spin configurations. The solid line in the upper panel is the same as in Figs. 3–5. Clearly, its overall upward trend with H is purely accidental.

below. From now on we present results based on Δt being equal to 1000 only.

The way H is incremented determines $\sigma(H)$ in a major fashion. This is shown in Fig. 4 where H is incremented from 0 to 1 either in 40 or in 20 steps. The two curves show little correlation with each other.

Magnetoconductance depends on the starting spin configuration in an even more striking way. Figure 5 shows the solid line of Figs. 3–5 in a companion of three other $\sigma(H)$ curves derived for different starting spin configurations, all obtained at $T=0.4J_0/k_B$. The four lines are totally uncorrelated and testify to the very sensitive way the overall spin pattern determines the conductivity. This pattern depends much more on history of cooling than on what a magnetic field does to it.

V. TEMPERATURE DEPENDENCE OF MAGNETOCONDUCTANCE FLUCTUATIONS

In our previous paper we have studied the rms fluctuations in conductivity on the Monte Carlo trajectory. These fluctuations decreased monotonically on lowering T (without any anomaly at the freezing temperature) because of a reduction in disorder. We now consider what happens to the fluctuations in the time-averaged conductivity as plotted against H . For a given Δt the time averaging should produce substantial smoothing effects at high temperatures (rapid changes in instantaneous values of σ cancel each other in the average). At low temperatures, however, when relaxation is slow, the time averaging is still restricted to one or several “valleys” the features of which are strongly reflected in each instantaneous σ . Thus we expect the rms fluctuations in magnetoconductance to behave in an opposite way to that found for the thermal noise: the amplitude of these fluctuations should increase on cooling.

This is indeed found as demonstrated in Figs. 6–8.

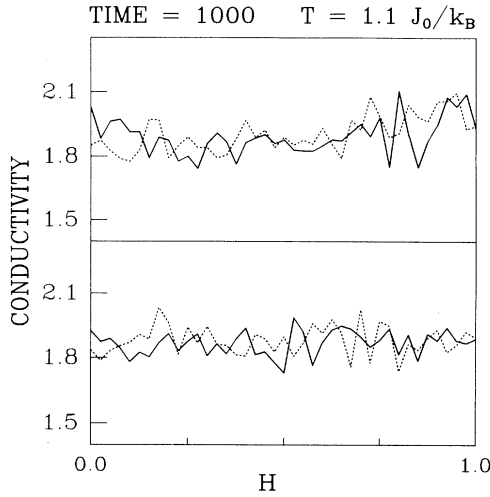


FIG. 6. Same as in Fig. 6 but for $T=1.1J_0/k_B$, i.e., just above the freezing temperature.

Figures 6 and 7 are the companions to Fig. 5. They show $\sigma(H)$ for four starting spin configurations at temperatures 1.1 and $3J_0/k_B$, respectively. The amplitude of the magnetoconductance fluctuations clearly goes down on heating. At $T=3J_0/k_B$ $\sigma(H)$ is flat and almost featureless. Results on the rms fluctuations in $\sigma(H)$ at various temperatures are gathered in Fig. 8 and contrasted to the behavior of the fluctuations due to the thermal noise. The magnetoconductance fluctuations depend on the time-averaging interval. The longer the Δt , the smaller the fluctuations. It is conceivable that for an infinite Δt the results would merge to a horizontal line with zero fluctuations. The point, however, is that in spin glasses one never reaches “infinite” times and a kink should be observed. Longer Δt 's should bring the kink closer to the

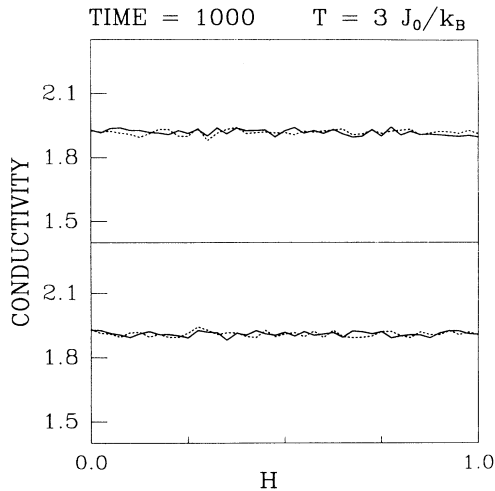


FIG. 7. Same as in Fig. 6 but for $T=3J_0/k_B$, i.e., high in the paramagnetic region.

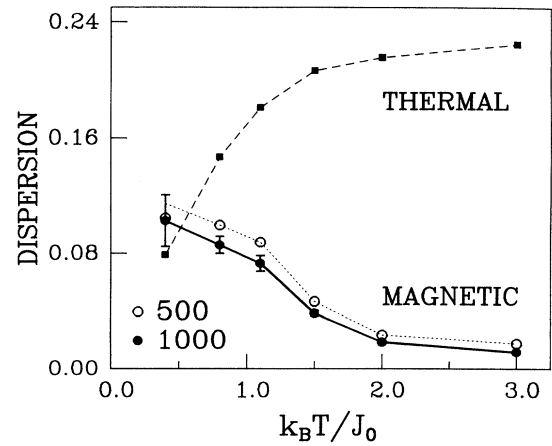


FIG. 8. Temperature dependence of the magnetoconductance fluctuations. The rms amplitude of fluctuations was obtained from 10 different runs at each T (all obtained from cooling down from $T=3J_0/k_B$). The field was incremented in 40 steps. The solid line is for $\Delta t=1000$ and the dotted one for $\Delta t=500$. The dashed line at the top shows the rms fluctuations due to thermal noise (in a time interval). This was obtained in the same runs which were used to determine the two lower curves. There is essentially no Δt dependence in the thermal noise.

freezing temperature. The predicted increase in the amplitude of magnetoconductance fluctuations on cooling of spin glasses seems to be consistent with the experimental observations of de Vegvar⁷ which we indicated in the Introduction.

It is interesting to point out that the upward trend in magnetoconductance fluctuations on cooling is specific to spin glasses. Figures 9 and 10 show what happens in the case of uniform- J ferromagnet in which the critical temperature, T_c , is close to $4.5J/k_B$. We use $\Delta t=1000$ and show examples of the $\sigma(H)$ curves in Fig. 10. The fluc-

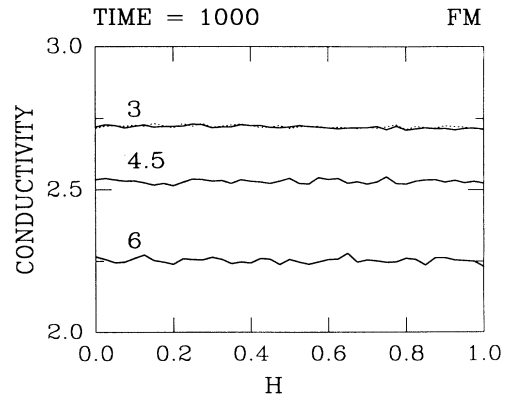


FIG. 9. Magnetoconductance in uniform ferromagnets for three temperatures indicated (in units J/k_B). All results are for two different starting spin configurations. These are seen at $T=3J_0/k_B$ as two lines: one solid and one dotted.

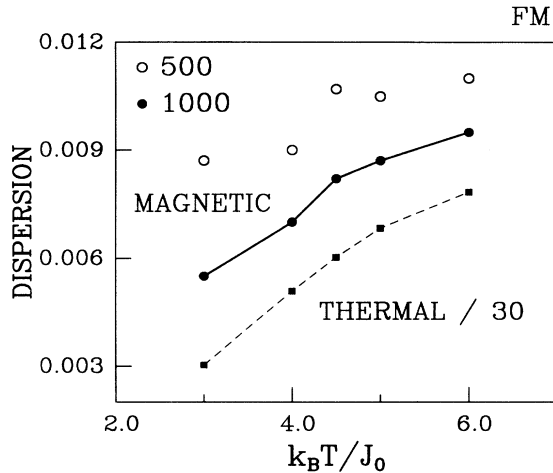


FIG. 10. Temperature dependence of magnetoconductance fluctuations in ferromagnets. The values of Δt are indicated next to the symbols used. The thermal fluctuations are also shown for a comparison. The scale is modified by the factor of 30.

tuations are much smaller due to the more strongly aligning effect of the field and there is a slight dependence on starting spin configurations at very low T . But at low T the alignment is close to perfect so the fluctuations go down with a decreasing T , as seen in Fig. 10.

VI. IRREVERSIBILITIES RELATED TO MAGNETIC FIELD

Suppose now that we prepare the system at a low temperature, like $0.4J_0/k_B$, and at zero field. We store some spin configuration and calculate $\sigma(H)$ and $\sigma(-H)$ both generated from the stored configuration (this can be done on the computer but probably not in the experiment). The resulting magnetoconductances are shown in Fig. 11.

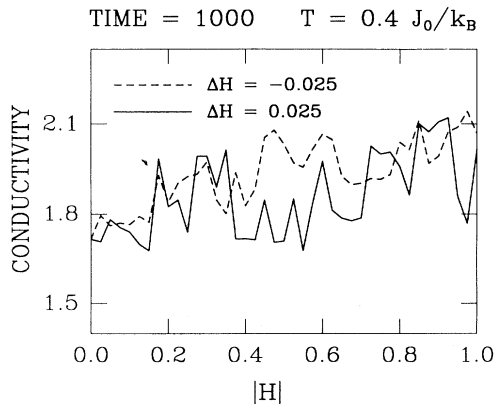


FIG. 11. Conductivity vs $|H|$ for two situations: the solid line (same as in Figs. 3–7) is for H incremented from 0 to 1 in 40 steps; the dashed line is for H decremented from 0 to -1 also in 40 steps. One starting spin configuration is considered.

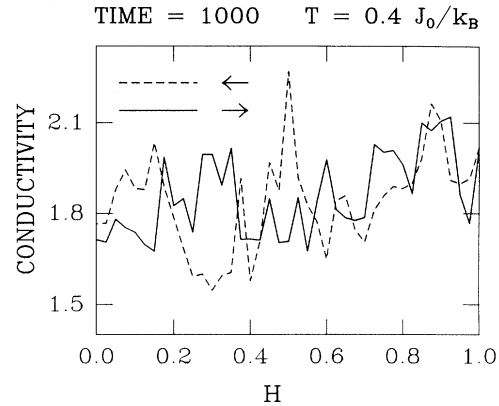


FIG. 12. Conductivity in field-cycling processes. The solid line corresponds to H incremented from 0 to 1 in 40 steps (same solid line as in Figs. 3–7) and the dashed line corresponds to H decremented from 1 to 0. The cycling is done at $T=0.4J_0/k_B$ and $\Delta t=1000$.

We find the two curves to be uncorrelated [the dispersion in $\sigma(H)-\sigma(-H)$ is $\sqrt{2}$ times the dispersion in $\sigma(H)$]. Thus extracting a “common part” from $\sigma(H)-\sigma(-H)$ appears to be pointless.

Consider now field-cycling experiments. Suppose we increase the field H from 0 to 1 and then reduce H back to 0 starting from the final spin configuration generated in the field-up process. Would the field-up curve resemble the field-down portion? Figure 12, for $T=0.4J_0/k_B$, shows that there is no resemblance whatsoever. The lack of reversibility is present even in the paramagnetic region, as shown in Fig. 12 for $T=3J_0/k_B$.

The general conclusion from our results is that spin glasses should be very difficult objects for experimental studies because reproducibility of the measurements is not expected to take place. There would be no way of telling what fluctuations are due to the experimental environment and what fluctuations are intrinsic to the system. Several experiments,^{8,11,12} however, report field cycling curves which are either quite reproducible, or to a good extent reproducible.⁷ The discrepancy between our results and experiments could be due to many reasons. Here we list several possibilities.

(1) When averaging over time scales which are orders of magnitude longer than studied here, the reproducibility could be effectively introduced because very gross features of the free-energy landscape might turn out to affect the resulting time-averaged conductivity. If this possibility is the correct one then its theoretical demonstration would be challenging. If few details of the spin structure survive the long time averaging of conductance then this approach may not be useful in attempting to see chaos in spin glasses.

(2) Because of a small number of lattice spins present in actual samples, or because of the nanostructurization procedure employed, the experimental systems are not really spin glassy: maybe they are disordered but not in the spin-glass regime. Signatures of the spin-glass regime, such as a violation of the Onsager-Büttiker symme-

try relations,^{7,15} might be caused by other effects, e.g., by a nonlinearity in the current-voltage characteristics.

(3) The lattice Zeeman effects are indeed irreversible but the magnetoresistance is dominated by the orbital effects which may depend on the lattice spins very weakly and be reversible. The Zeeman part would just act as an extra noise that shortens the phase-breaking length.

(4) The observed field-induced fluctuations of the conductance are caused by the spin effects. However, the dominant mechanism is not the change in the lattice spin configuration but the spin-splitting-induced redistribution of the electrons between the spin subbands and the corresponding shift of the Fermi energy with respect to the energy levels of the system.

(5) The field is, in practice, so strong that the exchange couplings, and thus glassy effects, act as minor perturbations.

(6) There could be more reproducibility in the case of continuous symmetry spins, as opposed to the Ising ones in which all changes are abrupt.

On more general grounds, however, the lack of *exact* reproducibility in spin glasses should be expected as a rule and its presence as a surprise.

ACKNOWLEDGMENTS

One of the authors (M.C.) thanks M. Weisseman, P. G. N. de Vegvar, and V. Chandrasekhar for useful discussions. This research was supported by KBN Grant Nos. 20466-91-01 (T.D.) and 2 P302 127 07 (M.C.). Generous and extended support by Rutgers University in providing computational facilities is warmly appreciated.

¹*Physics and Technology of Submicron Structures*, edited by H. Heinrich, G. Bauer, and F. Kuchar, Springer Series in Solid-State Sciences Vol. 83 (Springer-Verlag, Berlin, 1988).

²IBM J. Res. Develop. **32** (1988); B. L. Altshuler and B. I. Shklovskii, Zh. Eksp. Teor. Fiz. **91**, 220 (1986) [Sov. Phys. JETP **64**, 127 (1986)]; P. A. Lee, A. D. Stone, and H. Fukuyama, Phys. Rev. B **35**, 1039 (1987).

³B. L. Altshuler and B. Spivak, Pis'ma Zh. Eksp. Teor. Fiz. **42**, 363 (1985) [JETP Lett. **42**, 477 (1986)]; see also V. I. Fal'ko, J. Phys.: Condens. Matter **4**, 3943 (1992).

⁴S. Feng, A. J. Bray, P. A. Lee, and M. A. Moore, Phys. Rev. B **36**, 5624 (1987).

⁵N. E. Israeloff, M. B. Weissman, G. J. Nieuwenhuys, and J. Kosiorowska, Phys. Rev. Lett. **63**, 794 (1989); N. E. Israeloff, G. B. Alers, and M. B. Weissman, Phys. Rev. B **44**, 12 613 (1991); M. B. Weissman, Rev. Mod. Phys. **65**, 829 (1993).

⁶M. Cieplak, B. R. Bulka, and T. Dietl, Phys. Rev. B **44**, 12 337 (1991).

⁷P. G. N. de Vegvar, L. P. Levy, and T. A. Fulton, Phys. Rev. Lett. **64**, 2380 (1991); in *Science and Technology and Mesoscopic Structures*, edited by S. Namba *et al.* (Springer, Tokyo, 1992), p. 33.

⁸G. Grabecki, A. Lenard, W. Plesiewicz, J. Jaroszynski, T. Skoskiewicz, T. Dietl, E. Kaminska, A. Piotrowska, and B. Bulka, Acta Phys. Pol. **80**, 307 (1991); T. Dietl, G. Grabecki, and J. Jaroszynski, Semicond. Sci. Technol. **8**, S141 (1993).

⁹A. Benoit, D. Mailly, P. Perrier, and P. Nedellec, Superlatt. Microstructures **11**, 313 (1992).

¹⁰C. Van Haesendonck, H. Vloeberghs, Y. Bruynseraede, and R. Jonckheere, in *Nanostructure Physics and Fabrication*,

edited by M. A. Reed and W. P. Kirk (Academic, Boston, 1989), p. 467.

¹¹V. Chandrasekhar (private communication).

¹²G. Grabecki, J. Jaroszynski, J. Lennard, A. Plesiewicz, W. Skoskiewicz, T. Dietl, E. Kaminska, A. Piotrowska, G. Springholz, and G. Bauer, in *Proceedings of the 21st International Conference on the Physics of Semiconductors*, edited by P. Jiang and H.-Z. Zheng (World Scientific, Singapore, 1992), p. 1407.

¹³G. Grabecki, T. Dietl, W. Plesiewicz, A. Lennard, T. Skoskiewicz, E. Kaminska, and A. Piotrowska, Physica B **194-196**, 1107 (1994).

¹⁴S. Hershfield, Ann. Phys. **196**, 12 (1989); Phys. Rev. B **44**, 3320 (1991).

¹⁵P. G. N. de Vegvar and T. A. Fulton, Phys. Rev. Lett. **71**, 3537 (1993).

¹⁶A. J. Bray and M. A. Moore, in *Heidelberg Colloquium on Glassy Dynamics*, edited by L. Van Hemmen and I. Morgenstern (Springer, Berlin, 1987), p. 121; A. J. Bray, Comments Condens. Matter Phys. **14**, 21 (1988).

¹⁷K. Binder and A. P. Young, Rev. Mod. Phys. **58**, 801 (1986).

¹⁸A. D. Stone, *Physics and Technology of Submicron Structures* (Ref. 1), p. 108.

¹⁹R. J. Elliot, J. A. Krumhansl, and P. L. Leath, Rev. Mod. Phys. **46**, 465 (1974).

²⁰P. A. Lee and D. S. Fisher, Phys. Rev. Lett. **47**, 882 (1981).

²¹E. N. Economou, *Green's Functions in Quantum Physics* (Springer, Berlin, 1979).

²²A. MacKinnon and B. Kramer, Z. Phys. B **53**, 1 (1983); B. Bulka, M. Schreiber, and B. Kramer, *ibid.* **66**, 21 (1987).